Math. Model. Nat. Phenom. 19 (2024) 18
https://doi.org/10.1051/mmnp/2024016

Mathematical Modelling of Natural Phenomena
www.mmnp-journal.org

ALTERNATIVE STABLE STATES AND DISEASE INDUCED EXTINCTION

Dinesh Ekanayake[1,2,*], Hunter La Croix[3] and Amy Ekanayake[1]

Abstract. In this research, we study a generalization of the SIR epidemic model to observe disease-induced extinction in the presence of alternative stable states. We model per capita reproduction and mortality rates as functions of both population density and external indicators reflecting temporal resource variations that impact stable states. We then obtain conditions to guarantee a unique global solution for the SIR model when the rate functions are discontinuous. We further obtain conditions for the stability of two states when the external indicators are assumed to be constant. We use both deterministic and stochastic epidemic simulations to analyze models with alternative stable states for real mammalian populations. Through numerical examples, we show that changes in external indicators can, in fact, lead to the collapse of a population subject to an epidemic. However, we find a high probability of species survival in the presence of environmental stochasticity, even when the corresponding deterministic models predict extinction of the host population.

Mathematics Subject Classification. 92D25, 92D30, 60H10, 34A36, 34C60.

Received June 20, 2023. Accepted June 24, 2024.

1. Introduction

In ecology, alternative stable states refers to the occurrence of multiple stable states of a ecosystem. Ecosystems may transition from one state to another by a strong perturbation in the variables or due to a temporary change in ecosystem parameters [1, 2]. The study of alternative stable states can reveal warning signs of catastrophic shifts, such as population collapses, so that ecosystems can be managed [3–5]. Infectious diseases can induce species decline and extinction due to underlying alternative stable states and fluctuations in environmental conditions [6–8]. Changes in density-dependent and trait-mediated fitness components, as well as in abiotic factors that represent resource limitations, can precipitate a population collapse. However, existing epidemic models primarily quantify only density-driven stable states [9–11]. In this paper, we generalize SIR epidemic models (Susceptible, Infectious, and Removed) to incorporate alternative stable states arising from Allee effects and temporal variations in demographic rates due to changes in resource availability and allocations. The most

Keywords and phrases: Allee effect, resource indicators, discontinuous differential equations, stochastic differential equations.

[1] Department of Mathematics & Philosophy, Western Illinois University, 1 University Circle, Macomb, IL 61455, USA.
[2] The Preston M. Green Department of Electrical & Systems Engineering, Washington University in St. Louis, 1 Brookings Drive, St. Louis, MO 63130, USA.
[3] The Department of Applied and Computational Mathematics and Statistics, University of Notre Dame, 102G Crowley Hall, Notre Dame, IN 46556, USA.

* Corresponding author: db-ekanayake@wiu.edu

consequential feature of the proposed generalization is its capacity for incorporating piecewise continuous regression models for the fitness components and various resource indicators to evaluate the potential for population collapse under the strain of an infectious disease (see Sect. 3).

The Allee effect is a positive correlation between population density and mean individual fitness, such that the per capita growth rate of populations at low densities increases with an increase in density [12, 13]. Allee effects may be caused by several mechanisms that influence changes in individual fitness. A reduced reproduction rate due to the failure to locate mates is one such mechanism [13–16]. A per-capita increase in vigilance efforts for predators at lower densities can impact both reproduction and survival rates [17, 18]. Disruptions to cooperative behaviors, such as group foraging, hunting in packs, and interactions of collectively moving prey, lead to reduced survival rates in small populations [19–21]. Hence, the Allee effect is an important phenomenon to include in epidemic models when epidemics tend to decrease population densities or social interactions.

Population density is the primary resource indicator utilized in population models, as it is frequently assumed to influence fitness components [22]. Density-dependent reproduction can be observed in energy conserving life-history strategies, such as when an increased density results in an increased age of reproductive maturity and reduced pregnancy rates [23–26]. A decrease in survival rates may be observed near carrying capacity, the maximum sustainable population for a given environment [27]. Such variations in fitness components govern the stable states of a healthy population and may be modeled using population density and resource indicators [28]. Although decreased population growth at lower densities characterizes the Allee effect, this alone may not result in the existence of multiple stable states (weak Allee effect). A coupling of Allee effects with resource limitations may be necessary to drive a low density population to extinction. Trait-mediated fitness components may be strongly related to both spatial and temporal resource variation even at low densities [29, 30]. Species characteristics (such as morphology and development) and abiotic factors (such as soil, water, temperature) that represent resource availability may be necessary for predicting alternative stable states.

When population densities are below the ecological carrying capacity, the correlation between density and resource availability may be insignificant. Here we are particularly interested in including observations that can measure temporal variations in resource density and allocation among individuals in epidemic models, which we call resource indicators. An ongoing disease can impact physical development and resource allocation among infected individuals, producing changes in mean fitness components. Also, changes in weather patterns can impact the survival of a disease. See Section 3 for some examples. The effects of these factors can be characterized by resource indicators, including periodic measurements of developmental and abiotic factors, such as body mass, snow depth, average annual minimum winter temperatures, and summer precipitation [31–38]. Approximations for such discrete-time sequences of data points may naturally be chosen as piecewise constant functions or may be related to fitness components *via* regression models [28]. There are many region-specific resource indicators that are constants, such as the aridity index, Köppen–Geiger climate classifications, and United States Department of Agriculture (USDA) hardiness zones. These spatial variations may be included in models without explicitly changing the model form (see [28]).

Many studies have analyzed epidemiological systems with alternative stable states driven by Allee effects [9–11, 39, 40]. Most models generate stable states by defining the dynamics such that the total population exhibits the strong Allee effect, given by $\mathrm{d}N/\mathrm{d}t = \mathrm{d}N(N/k_1 - 1)(1 - N/k_2)$, where N is the population density and k_1, k_2 are constants. While such models mimic the impact of reduced reproduction, they cannot incorporate the impact of variations in resource allocations that may produce alternate stable states. In this paper, we study the SIR model with generalized reproduction and mortality functions to facilitate incorporating various ecological mechanisms that can govern the stable states. We model per capita reproduction and mortality rates as functions of population density and phenotypic indicators or other external observations that reflect temporal resource variations and allocation. The resulting rate functions may be discontinuous and we obtain conditions that guarantee the existence of a unique global solution for the model. We further obtain parameter constraints that govern the existence of alternative stable states and the basic reproduction number for the model when the external indicators are constant.

Environmental stochasticity refers to spatio-temporal fluctuations in environmental conditions. These changes lead to temporal changes in the rates of events, such as in reproduction and death rates. Even when the

population is not particularly small, environmental stochasticity contributes to extinction [41]. It is important to include environmental stochasticity to satisfactorily explain the behavior of the spread of a disease through a population exhibiting Allee effects. In this paper, we use both deterministic and stochastic epidemic simulations to analyze models with alternative stable states. Through numerical examples, we show that changes in resource indicators can, in fact, lead to the collapse of a population subject to an epidemic. We find a high probability of species survival in the presence of environmental stochasticity, even when the corresponding deterministic models predict extinction of the host population. Environmental stochasticity is apt to force the collapse of the infected class before a collapse of the susceptible class, facilitating a revival of the population (See Sect. 3).

2. Generalized SIR model

We first establish notation and terminology. Spaces $AC(\Omega)$ and $BC_{pm}(\Omega)$ denote absolute continuous functions and bounded piecewise monotone continuous functions on Ω, respectively, where $\Omega \subset [0,\infty)$ is an interval. We define $\|x\|_\infty = \sup_{t\in[0,T]} \|x(t)\|$, where we take $\|x(t)\| = \sum_{i=1}^{p} |x_i(t)|$. Let $S(t)$, $I(t)$, and $R(t)$ be the density of individuals at time t in the susceptible, infectious, and immune classes, respectively, and $N(t)$ be the host population density at time t: $N(t) = S(t) + I(t) + R(t)$. For simplicity, we drop the function notation for S, I, R, and N. Function $\sigma(t)$ represents temporal variations and allocations of resources. We define per capita reproduction and mortality rates as functions of both $\sigma(t)$ and population density: $\mathcal{B}(\sigma(t), N)$ and $\mathcal{D}(\sigma(t), N)$, respectively.

Function $\sigma(t)$ may be a piecewise constant approximation for the resource factors and may thus produce right hand side discontinuities in the SIR model. To guarantee a unique solution, we make the following assumptions for modeling the spread of disease.

$\mathcal{A}1$: Function $\sigma(t)$ is a density-independent input variable to the system, $\sigma(t) \in BC_{pm}[0,\infty)$, and $\sigma(t) \in [\sigma_*, \sigma^*]$ for some $\sigma_*, \sigma^* \in \mathbb{R}$.

$\mathcal{A}2$: Newborns are susceptible at birth. The per-capita birth rate $\mathcal{B}(\sigma(t), N) \geq 0$ for each $(\sigma(t), N)$. The map $\sigma(\cdot) \mapsto \mathcal{B}(\sigma(\cdot), N)$ is continuous and monotone increasing for each N. The map $N \mapsto \mathcal{B}(\sigma(t), N)$ is differentiable with respect to N for each $\sigma(t)$ and $\partial\mathcal{B}(\sigma(t), N)/\partial N$ is bounded on each compact set of the domain.

$\mathcal{A}3$: The per-capita rate of death may be higher among infectious individuals: $\mathcal{D}(\sigma(t), N)$ for the susceptible and immune classes and $\mathcal{D}_I(\sigma(t), N)$ for the infectious class, where $\mathcal{D}_I(\sigma(t), N) \geq \mathcal{D}(\sigma(t), N) > 0$ for each $(\sigma(t), N)$. The maps $\sigma(\cdot) \mapsto \mathcal{D}(\sigma(\cdot), N)$ and $\sigma(\cdot) \mapsto \mathcal{D}_I(\sigma(\cdot), N)$ are continuous and monotone decreasing for each N. The maps $N \mapsto \mathcal{D}(\sigma(t), N)$ and $N \mapsto \mathcal{D}_I(\sigma(t), N)$ are differentiable with respect to N for each $\sigma(t)$ and their partial derivatives are bounded on each compact set of the domain, with $\partial\mathcal{D}_I(\sigma(t), N)/\partial N \geq \partial\mathcal{D}(\sigma(t), N)/\partial N$.

$\mathcal{A}4$: The per-capita rate that susceptible individuals become infected is βI for host-to-host transmission. The per-capita rate at which susceptible individuals become vaccinated is constant, v.

$\mathcal{A}5$: The per-capita rate of recovery is constant, γ. The proportion of recovered individuals that return to the susceptible class is $\alpha \in [0,1]$ and the remaining recovered individuals become immune to the disease. If infectious individuals are infectious for life, $\gamma = 0$.

2.1. ODE model

The ordinary differential equation (ODE) model satisfying assumptions $\mathcal{A}1 - \mathcal{A}5$ is given by

$$\frac{\mathrm{d}S}{\mathrm{d}t} = \mathcal{B}(\sigma(t), N)N - (\mathcal{D}(\sigma(t), N) + v + \beta I)\, S + \alpha\gamma I \tag{2.1}$$

$$\frac{\mathrm{d}I}{\mathrm{d}t} = \beta SI - (\mathcal{D}_I(\sigma(t), N) + \gamma)\, I \tag{2.2}$$

TABLE 1. Description of the functions in equation (2.4) modeling deer reproduction.

Function	Definition
$\overline{m}(N)$	The mean body weight of female deer as a differentiable and monotone function of N.
m_z^*	The critical mean female weight for breeding in zone z.
$f(z)$	A nonnegative real valued function of zone z representing the impact of plant survival on reproduction.
$\phi(t)$	An indicator function defining the birth season.
$p(t)$	The proportion of juveniles surviving to weaning age as a piecewise continuous function of t.

$$\frac{\mathrm{d}R}{\mathrm{d}t} = vS + (1-\alpha)\gamma I - \mathcal{D}(\sigma(t), N)R. \tag{2.3}$$

Here $\mathcal{B}(\sigma(t), N)$, $\mathcal{D}(\sigma(t), N)$, and $\mathcal{D}_I(\sigma(t), N)$ may represent an intricate set of functions, provided that they satisfy the assumptions. For example, consider the deer reproduction function given in [28], adjusted to include seasonal births:

$$\mathcal{B}(\overline{m}(N), z, t) = \begin{cases} \dfrac{\alpha p(t) f(z)(\overline{m}(N) - m_z^*)}{1 + \beta f(z)(\overline{m}(N) - m_z^*)}\phi(t), & \text{if } \overline{m}(N) > m_z^*, \\ 0, & \text{otherwise,} \end{cases}, \tag{2.4}$$

where α, β are nonnegative constants and z is the USDA hardiness zone. Each hardiness zone represents a geographic area that is defined by its average annual minimum winter temperature, a key factor in the survival of many plants. See Table 1 for the definition of functions $f(z)$, $\overline{m}(N)$, m_z^*, $\phi(t)$, and $p(t)$. Functions $f(z)$, $\overline{m}(N)$ and $p(t)$ may represent regression models. Notice that one may choose $p(t)\phi(t)$ as $\sigma(t)$. Then for any given region, $\mathcal{B}(\overline{m}(N), z, t)$ satisfies assumptions $\mathcal{A}1$ and $\mathcal{A}2$. Here we prove all the results for a single resource function ($\sigma(t)$), though results can be directly extended to any number of resource functions.

Define $\boldsymbol{x} = [x_1, x_2, x_3]^{\mathrm{T}}$ so that x_i represents S, I and R for $i = 1, 2$ and 3, respectively. For simplicity, System (2.1)–(2.3) may be represented in the form $\dfrac{\mathrm{d}x_j}{\mathrm{d}t} = g_j(\sigma(t), \boldsymbol{x})$, where $g_j(\sigma(t), \boldsymbol{x}) = g_j(\sigma(t), S, I, R)$ for each j. We define the growth rate of the population by

$$f(\sigma(t), N) = \mathcal{B}(\sigma(t), N)N - \mathcal{D}(\sigma(t), N)N.$$

We first show the existence and uniqueness of a nonnegative solution for any nonnegative initial conditions. From Hypothesis $\mathcal{A}1$, $\sigma(t)$ is continuous almost everywhere. Here we seek $\boldsymbol{x} \in AC[0, \infty)$ satisfying equations (2.1)–(2.3) except on a Lebesgue measure zero set.

Lemma 2.1. *If there exists $(\tilde{\sigma}, N^*) > 0$ such that $\mathcal{B}(\sigma(t), N^*) - \mathcal{D}(\sigma(t), N^*) < 0$ for all $\sigma(t) > \tilde{\sigma}$, then any solution $\boldsymbol{x}$ of System (2.1)–(2.3) with $\|\boldsymbol{x}(0)\| < N^*$ satisfies $\|\boldsymbol{x}\|_\infty < N^*$.*

Proof. Let $\Omega_j = \left\{\boldsymbol{x}(t) \in \mathbb{R}_+^3 \mid x_j(t) = 0\right\}$. It is straightforward to see that for all $\boldsymbol{x}(t) \in \Omega_j$, $\mathrm{d}x_j/\mathrm{d}t \geq 0$. Then the set $\mathbb{R}_+^3$ is positively invariant for the system. By summing equations (2.1)–(2.3),

$$\frac{\mathrm{d}N}{\mathrm{d}t} = f(\sigma(t), N) - \left(\mathcal{D}_I(\sigma(t), N) - \mathcal{D}(\sigma(t), N)\right) I. \tag{2.5}$$

From assumptions $\mathcal{A}2$ and $\mathcal{A}3$, $\mathcal{B}(\sigma(t), N) \leq \mathcal{B}(\sigma^*, N)$ and $\mathcal{D}(\sigma(t), N) \geq \mathcal{D}(\sigma^*, N)$, where σ^* is the upper bound for $\sigma(t)$ (Asm. $\mathcal{A}1$). Then $f(\sigma(t), N) \leq f(\sigma^*, N)$. Since $\mathcal{D}_I(\sigma(t), N) \geq \mathcal{D}(\sigma(t), N)$ and the system is positive

invariant, $\frac{\mathrm{d}N}{\mathrm{d}t} \le f(\sigma^*, N)$. Consider the comparison equation $y'(t) = f(\sigma^*, y)$, $y(0) = N(0)$. From assumptions $\mathcal{A}2$ and $\mathcal{A}3$, there exists $M > 0$ such that $|\mathrm{d}f(\sigma^*, y)/\mathrm{d}y| < M$ for any given compact set $[0, T] \times [0, \tilde{N}]$, where $\tilde{N} > N(0)$. From the mean value theorem, we have $|f(\sigma^*, y_1) - f(\sigma^*, y_2)| \le M|y_1 - y_2|$. Then $f(\sigma^*, y)$ is locally Lipschitz continuous and there exists a unique local solution $y(t) \in C^1([0, \tilde{t}])$ for some $[0, \tilde{t}]$ (by the Picard–Lindelöf theorem). Since $\sigma^* > \tilde{\sigma}$, $f(\sigma^*, N^*) < 0$. Therefore, $y'(t) < 0$ whenever $y(t) = N^*$. Using the continuity of $y'(t)$ and $y(0) < N^*$, we conclude that $y(t) < N^*$ for all t. From the continuation of the solution, $y(t)$ exists for all time. Now by comparison, any solution of equation (2.5) satisfies $N(t) < N^*$, and hence, $\|x(t)\| < N^*$ for all t, which concludes the proof. □

From Lemma 2.1, it is sufficient to consider $\boldsymbol{x}(t) \in \Omega_0 := \{\boldsymbol{y} \in \mathbb{R}^3_+ : \|\boldsymbol{y}\| < N^*\}$. Let $\Omega = [0, \infty) \times \Omega_0$. Define $F : \Omega \to \mathbb{R}^3$ by $F(t, \boldsymbol{x}) = [g_1(\sigma(t), \boldsymbol{x}), g_2(\sigma(t), \boldsymbol{x}), g_3(\sigma(t), \boldsymbol{x})]^T$.

Lemma 2.2. *Suppose the conditions in Lemma 2.1 are satisfied. Then the map $\boldsymbol{x} \mapsto F(t, \boldsymbol{x})$ is Lipschitz continuous for each t, with a uniform Lipschitz constant on Ω.*

Proof. Let $\boldsymbol{x}_1 = [S_1, I_1, R_1]^T$, $\boldsymbol{x}_2 = [S_2, I_2, R_2]^T$, $N_1 = S_1 + I_1 + R_1$ and $N_2 = S_2 + I_2 + R_2$. From assumptions $\mathcal{A}2$ and $\mathcal{A}3$, $\mathcal{B}(\sigma(t), N)$, $\mathcal{D}(\sigma(t), N)$, $\mathcal{D}_I(\sigma(t), N)$, and their partial derivatives with respect to N are bounded on $[\sigma_*, \sigma^*] \times [0, N^*]$. Let

$$L_1 = N^* \left\| \frac{\partial \mathcal{D}}{\partial N} \right\|_\infty + N^* \left\| \frac{\partial \mathcal{B}}{\partial N} \right\|_\infty + \|\mathcal{B}\|_\infty \quad \text{and} \quad L_2 = \max\left\{ N^* \left\| \frac{\partial \mathcal{D}}{\partial N} \right\|_\infty, N^* \left\| \frac{\partial \mathcal{D}_I}{\partial N} \right\|_\infty \right\}.$$

Then

$$|g_1(\sigma(t), \boldsymbol{x}_1) - g_1(\sigma(t), \boldsymbol{x}_2)| \le L_1|N_1 - N_2| + (\|\mathcal{D}\|_\infty + v + \beta N^*)\,|S_1 - S_2| + (\alpha\gamma + \beta N^*)\,|I_1 - I_2|, \tag{2.6}$$

$$|g_2(\sigma(t), \boldsymbol{x}_1) - g_2(\sigma(t), \boldsymbol{x}_2)| \le L_2|N_1 - N_2| + \beta N^*|S_1 - S_2| + (\|\mathcal{D}_I\|_\infty + \gamma + \beta N^*)\,|I_1 - I_2|, \tag{2.7}$$

$$|g_3(\sigma(t), \boldsymbol{x}_1) - g_3(\sigma(t), \boldsymbol{x}_2)| \le L_2|N_1 - N_2| + v|S_1 - S_2| + \|\mathcal{D}\|_\infty\,|R_1 - R_2| + (1 - \alpha)\gamma|I_1 - I_2|. \tag{2.8}$$

By summing inequalities (2.6)–(2.8) and using $|N_1 - N_2| \le \|\boldsymbol{x}_1 - \boldsymbol{x}_2\|$,

$$\|F(t, \boldsymbol{x}_1) - F(t, \boldsymbol{x}_2)\| \le (L_1 + 2L_2 + \|\mathcal{D}_I\|_\infty + 2v + 2\beta N^* + 2\gamma)\|\boldsymbol{x}_1 - \boldsymbol{x}_2\|.$$

Then $F(t, \boldsymbol{x})$ is Lipschitz continuous for each t, with a uniform Lipschitz constant $L_1 + 2L_2 + \|\mathcal{D}_I\|_\infty + 2v + 2\beta N^* + 2\gamma$. □

Theorem 2.3. *If there exists $(\tilde{\sigma}, N^*) > 0$ such that $\mathcal{B}(\sigma(t), N^*) - \mathcal{D}(\sigma(t), N^*) < 0$ for all $\sigma(t) > \tilde{\sigma}$, then System (2.1)–(2.3) with a given initial condition $\boldsymbol{x}(0)$ satisfying $\|\boldsymbol{x}(0)\| < N^*$ possesses a unique global solution.*

Proof. Since $\sigma(t)$ is piecewise continuous, the map $t \mapsto F(t, \boldsymbol{x})$ is measurable for each x. From Lemma 2.2, the map $\boldsymbol{x} \mapsto F(t, \boldsymbol{x})$ is Lipschitz continuous for each t, with a uniform Lipschitz constant. From the continuity, functions $\mathcal{B}$, $\mathcal{D}$, and $\mathcal{D}_\mathcal{I}$ achieve their extrema on $\overline{\Omega_0} \times [\sigma_*, \sigma^*]$. It follows that there exists an $M_i > 0$ such that $|g_i(\sigma(t), \boldsymbol{x})| < M_i$ for all $(t, \boldsymbol{x}) \in \Omega$ and for each $i = 1, 2, 3$. Then for each compact set U of Ω, $\|F(t, \boldsymbol{x})\| < C_0$, where $C_0 = M_1 + M_2 + M_3$. Since C_0 is integrable on U, function $F(t, \boldsymbol{x})$ satisfies the Carathéodory conditions on Ω. Then from the classical theorem of Carathéodory (see, for example, Thm. 5.3 of [42]), System (2.1)–(2.3) possesses a unique local solution passing through (S_0, I_0, R_0). Further, from Lemma 2.1, the solution does not reach the boundary of any open set containing Ω. Then $[0, T]$ is not a maximum interval of existence for any T (the converse of Thm. 5.2 of [42]). Therefore, the solution is global. □

From equation (2.5) combined with assumptions $\mathcal{A}2$ and $\mathcal{A}3$, one can see that if, for a given $\tilde{\sigma}$, $\mathcal{B}(\tilde{\sigma}, 0) - \mathcal{D}(\tilde{\sigma}, 0) < 0$, then there exists a basin of attraction for $N = 0$ for any $\sigma(t) < \tilde{\sigma}$. Then the origin $\boldsymbol{x}(t) = \boldsymbol{0}$ is a

local attractor for System (2.1)–(2.3). Suppose $U \in \mathbb{R}^3_+$ is a neighborhood of $\mathbf{0}$ such that

$$\mathcal{B}(\sigma(t), N) - \mathcal{D}(\sigma(t), N) - (\mathcal{D}_I(\sigma(t), N) - \mathcal{D}(\sigma(t), N))\,\rho_I < 0 \tag{2.9}$$

for all $(\boldsymbol{x}(t), \sigma(t)) \in U \times [\sigma_*, \tilde{\sigma}]$, where $\rho_I = I/N$ is the proportion of infected individuals. Then the basin of attraction for $\mathbf{0}$ contains U. Therefore, the extinction dynamics in the presence of a disease are governed by the birth rate, death rate, and infection parameters, as well as the temporal evolution of $\sigma(t)$. Also, if the birth and death rates satisfy assumptions $\mathcal{A}1$–$\mathcal{A}3$, and the host population adheres to a differential equation described by equation (2.5), then Lemma 2.1 through Theorem 2.3 apply to any extension of the SIR model. These extensions encompass compartmental models such as susceptible-exposed-infected-recovered (SEIR) and susceptible-infected-recovered-vaccinated-deceased (SIRVD).

2.2. Stability of alternative equilibria for constant $\sigma(t)$

Assuming an environment with abundant resources, here we establish conditions for the existence of alternative stable states for a constant $\sigma(t)$. In this case, $\mathcal{B}(\sigma(t), N), \mathcal{D}(\sigma(t), N)$, and $\mathcal{D}_I(\sigma(t), N)$ are functions of N only and we drop $\sigma(t)$ from the notation throughout this section. System (2.1)–(2.3) with a constant $\sigma(t)$ possesses three equilibrium solutions.

(A) Trivial equilibrium: $S = I = R = 0$

(B) Disease-free equilibrium: $S_0 = \dfrac{\mathcal{B}(N_0)N_0}{\mathcal{D}(N_0) + v},\ I_0 = 0,\ R_0 = \dfrac{vS_0}{\mathcal{D}(N_0)},\ N_0 = S_0 + R_0$

(C) Endemic equilibrium: $S_e = \dfrac{\mathcal{D}_I(N_e) + \gamma}{\beta},\ I_e = \dfrac{\mathcal{B}(N_e)N_e - (\mathcal{D}(N_e) + v)S_e}{\mathcal{D}_I(N_e) + \gamma(1-\alpha)},\ R_e = \dfrac{vS_e + (1-\alpha)\gamma I_e}{\mathcal{D}(N_e)},$
$N_e = S_e + I_e + R_e$

The growth rate of the population with constant $\sigma(t)$ is given by $f(N) = (\mathcal{B}(N) - \mathcal{D}(N))\,N$. As we have seen, if $f'(0) = \mathcal{B}(0) - \mathcal{D}(0) < 0$, then the trivial equilibrium is stable. Next, we use linear stability analysis to check the local stability of the equilibria. The Jacobian matrix $J(S, I, R)$ of System (2.1)–(2.3) is given by

$$\begin{bmatrix} b(N) - \mathcal{D}(N) - v - \beta I - \mathcal{D}'(N)S & b(N) - \beta S + \gamma\alpha - \mathcal{D}'(N)S & b(N) - \mathcal{D}'(N)S \\ \beta I - \mathcal{D}'_I(N)I & \beta S - \mathcal{D}_I(N) - \gamma - \mathcal{D}'_I(N)I & -\mathcal{D}'_I(N)I \\ v - \mathcal{D}'(N)R & (1-\alpha)\gamma - \mathcal{D}'(N)R & -\mathcal{D}(N) - \mathcal{D}'(N)R \end{bmatrix},$$

where $b(N) = \mathcal{B}(N) + \mathcal{B}'(N)N$ and the derivatives of the birth and death rates are taken with respect to N. Theorem 2.4 provides conditions for stability of the disease-free and trivial equilibria.

Theorem 2.4. *Suppose $\sigma(t)$ is a constant and System (2.1)–(2.3) satisfies assumptions $\mathcal{A}1 - \mathcal{A}5$ and possesses a nontrivial disease-free equilibrium $(S_0, 0, I_0)$. If $f'(0) < 0$, $f'(N_0) < 0$ and*

$$\beta < \frac{(\mathcal{D}(N_0) + v)(\mathcal{D}_I(N_0) + \gamma)}{\mathcal{D}(N_0)N_0}, \tag{2.10}$$

then the trivial and disease-free equilibria are locally stable, where $N_0 = S_0 + R_0$.

Proof. The eigenvalues of $J(S_0, 0, R_0)$ are given by $\lambda_1 = \beta S_0 - \mathcal{D}_I(N_0) - \gamma, \lambda_2 = -\mathcal{D}(N_0) - v$, and $\lambda_3 = b(N_0) - \mathcal{D}(N_0) - \mathcal{D}'(N_0)N_0$. The rate of population change $\mathrm{d}N/\mathrm{d}t$ evaluated at the disease-free equilibrium implies $\mathcal{B}(N_0) = \mathcal{D}(N_0)$ (see Eq. (2.5)). Then from Equilibrium (B), $S_0 = \mathcal{D}(N_0)N_0/(\mathcal{D}(N_0) + v)$. Using equation (2.10), we obtain $\lambda_1 = \beta S_0 - \mathcal{D}_I(N_0) - \gamma < 0$. Since $\lambda_2 = -\mathcal{D}(N_0) - v < 0$ and $\lambda_3 = b(N_0) - \mathcal{D}(N_0) - \mathcal{D}'(N_0)N_0 = f'(N_0) < 0$, all the eigenvalues are negative, and thus, $(S_0, 0, R_0)$ is locally stable. Since $f'(0) < 0$, the trivial solution is also stable. □

The basic reproduction number obtained by the next-generation matrix method [43] is given by

$$R_0 = \frac{\mathcal{B}(N_0)N_0\beta}{(\mathcal{D}(N_0)+v)(\mathcal{D}_I(N_0)+\gamma)}. \tag{2.11}$$

Since $\mathcal{B}(N_0) = \mathcal{D}(N_0)$, $R_0 < 1$ does, in fact, correspond to Inequality (2.10).

Let E_{12} be the 3×3 single entry matrix unit. Define $J_0 = J(S_e, I_e, R_e) + (\mathcal{D}_I(N_e) - \mathcal{D}(N_e))\, E_{12}$. Then we have the following results for the endemic equilibrium.

Lemma 2.5. *Let (S_e, I_e, R_e) be the endemic equilibrium. If $f'(N_e) < 0$ and $I_e > 0$, then all the eigenvalues of J_0 have negative real parts.*

Proof. Let $a_{11} = b(N_e) - \mathcal{D}(N_e) - v - \beta I_e - \mathcal{D}'(N_e)S_e$ and $a_{12} = b(N_e) - \mathcal{D}(N_e) - (1-\alpha)\gamma - \mathcal{D}'(N_e)S$. From Equilibrium (C), $\beta S_e = \mathcal{D}_I(N_e) + \gamma$, and hence,

$$J_0 = \begin{bmatrix} a_{11} & a_{12} & b(N_e) - \mathcal{D}'(N_e)S_e \\ \beta I_e - \mathcal{D}_I'(N_e)I_e & -\mathcal{D}_I'(N_e)I_e & -\mathcal{D}_I'(N_e)I_e \\ v - \mathcal{D}'(N_e)R_e & (1-\alpha)\gamma - \mathcal{D}'(N_e)R_e & -\mathcal{D}(N_e) - \mathcal{D}'(N_e)R_e \end{bmatrix}.$$

Let $a = \beta I_e + \mathcal{D}_I(N_e) + v$ and $b = \beta I_e(\mathcal{D}(N_e) + (1-\alpha)\gamma) + (\mathcal{D}(N_e)+v)(\mathcal{D}_I(N_e) - \mathcal{D}(N_e))$. Then the eigenvalues of J_0 are given by $\lambda_1 = \frac{1}{2}\left(-a + \sqrt{a^2 - 4b}\right)$, $\lambda_2 = \frac{1}{2}\left(-a - \sqrt{a^2-4b}\right)$, and $\lambda_3 = b(N_e) - \mathcal{D}(N_e) - \mathcal{D}'(N_e)N_e$. From the lemma hypotheses, $\lambda_3 = f'(N_e) < 0$. If $a^2 - 4b < 0$ then $\sqrt{a^2-4b}$ is imaginary, so λ_1 and λ_2 have negative real part. Suppose $a^2 - 4b \geq 0$. In this case, it is immediately clear that $\lambda_2 < 0$. Since $a > 0$ and $b > 0$, we have $a^2 > a^2 - 4b$. Therefore, λ_1 and λ_2 are negative and thus have negative real part, as desired. □

If $\mathcal{D}_I(N_e) = \mathcal{D}(N_e)$, then $J_0 = J$ and the endemic equilibrium is stable. Next we prove the existence of some $\mathcal{D}_I$ satisfying $\mathcal{D}_I(N_e) > \mathcal{D}(N_e)$ that guarantees the local stability of the endemic equilibrium.

Theorem 2.6. *Suppose $\sigma(t)$ is a constant, and System (2.1)–(2.3) satisfies assumptions $\mathcal{A}1 - \mathcal{A}5$. If the conditions given in Lemma 2.5 are satisfied, then there exists $\delta > 0$ such that if $\mathcal{D}(N_e) \leq \mathcal{D}_I(N_e) < \mathcal{D}(N_e) + \delta$, then the trivial and endemic equilibria are locally stable.*

Proof. Let $\Gamma = \{z \in \mathbb{C} : \mathcal{R}e(z) < 0\}$ be the set of all complex numbers with negative real part, and let λ_i be any eigenvalues of J_0 with multiplicity μ_i. Since Γ is open and $\mathrm{Re}(\lambda_i) < 0$, there exists $\rho > 0$ such that the open ball $B(\lambda_i, \rho) \subset \Gamma$, and $\lambda_j \notin B(\lambda_i, \rho)$ for $i \neq j$. Let $P(\lambda)$ and $Q(\lambda)$ be the characteristic polynomials of J_0 and $J(S_e, I_e, R_e)$, respectively. Then

$$P(\lambda) - Q(\lambda) = (\mathcal{D}_I(N_e) - \mathcal{D}(N_e))\left(\beta I_0(\lambda + \mathcal{D}(N_e) + \mathcal{D}'(N_e)R_e) - \mathcal{D}_I'(N_e)I_e(\lambda + \mathcal{D}(N_e) + v)\right).$$

Define $M = \max\{|\beta I_0 - \mathcal{D}'(N_e)I_e|, |\beta I_0(\mathcal{D}(N_e) + \mathcal{D}'(N_e)R_e) - \mathcal{D}_I'(N_e)I_e(\mathcal{D}(N_e)+v)|\}$. Then the magnitudes of the coefficients of $P(\lambda) - Q(\lambda)$ are bounded by $M(\mathcal{D}_I(N_e) - \mathcal{D}(N_e))$. From the continuity of the eigenvalues, there exists ε_i such that $M(\mathcal{D}_I(N_e) - \mathcal{D}(N_e)) < \varepsilon_i$ and $B(\lambda_i, \rho)$ contains exactly μ_i roots of $Q(\lambda)$, counting multiplicities (see Thm. 3.1.1 of [44]). By choosing $\delta = \min_i \varepsilon_i/M$, we conclude that all the eigenvalues of $J(S_e, I_e, R_e)$ have negative real part whenever $\mathcal{D}_I(N_e) < \mathcal{D}(N_e) + \delta$. □

From Equilibrium (C), for $I_e > 0$ we must have $\beta > \dfrac{(\mathcal{D}(N_e)+v)(\mathcal{D}_I(N_e)+\gamma)}{\mathcal{B}(N_e)N_e}$. As I_e converges to 0, N_e converges to N_0. Then $R_0 > 1$ does, in fact, correspond to $I_e > 0$. However, an increased β results in an increased density of infected individuals. Then from Inequality 2.9, the basin of attraction of $\mathbf{0}$ increases as β increases. Subsequently, a large β may result in the collapse of a population, as we see in the examples.

TABLE 2. Transitions $\Delta\boldsymbol{X}(t) = \boldsymbol{X}(t+\Delta t) - \boldsymbol{X}(t)$, and the respective probabilities $\text{Prob}\{\Delta\boldsymbol{X}(t) \mid \boldsymbol{X}(t)\}$, where $\boldsymbol{e}_{X_i}$ has unity in the position corresponding to a variable X_i and zeros elsewhere and X_i represents the variables S, I, and R. It is assumed that $\Delta t > 0$ is sufficiently small so that $\text{Prob}\{\Delta\boldsymbol{X} = \boldsymbol{0} \mid \boldsymbol{X}(t)\} = \delta > 0$, where δ is the difference between unity and the sum of all probabilities listed in the table.

$\Delta\boldsymbol{X}$	$\text{Prob}\{\Delta\boldsymbol{X}(t) \mid \boldsymbol{X}(t)\}$	$\Delta\boldsymbol{X}$	$\text{Prob}\{\Delta\boldsymbol{X}(t) \mid \boldsymbol{X}(t)\}$
$\boldsymbol{e}_S$	$\mathcal{B}(\sigma(t), N)N\Delta t$	$\boldsymbol{e}_S - \boldsymbol{e}_I$	$\alpha\gamma I\Delta t$
$-\boldsymbol{e}_S$	$\mathcal{D}(\sigma(t), N)S\Delta t$	$\boldsymbol{e}_R - \boldsymbol{e}_I$	$(1-\alpha)\gamma I\Delta t$
$-\boldsymbol{e}_I$	$\mathcal{D}_I(\sigma(t), N)I\Delta t$	$\boldsymbol{e}_I - \boldsymbol{e}_S$	$\beta IS\Delta t$
$-\boldsymbol{e}_R$	$\mathcal{D}(\sigma(t), N)R\Delta t$	$\boldsymbol{e}_R - \boldsymbol{e}_S$	$vS\Delta t$

2.3. SDE model

Now consider an Itô stochastic differential equation (SDE) model corresponding to the deterministic model, having random variables

$$\boldsymbol{X} = \{X_i\}_{i=1}^3 = [S, I, R]. \tag{2.12}$$

The transitions $\Delta\boldsymbol{X}(t) = \boldsymbol{X}(t+\Delta t) - \boldsymbol{X}(t)$ for small Δt, and their corresponding probabilities $\text{Prob}\{\Delta\boldsymbol{X}(t) \mid \boldsymbol{X}(t)\}$, are given in Table 2.

The stochastic differential equation (SDE) model is formed as [45]:

$$\mathrm{d}\boldsymbol{X}(t) = \boldsymbol{f}(t, \boldsymbol{X})\mathrm{d}t + \mathbf{H}(t, \boldsymbol{X})\mathrm{d}\boldsymbol{W}(t),$$

where $\boldsymbol{f} = \dfrac{E(\Delta\boldsymbol{X})}{\Delta t}$, $\mathbf{H}\mathbf{H}^{\mathrm{T}} = \boldsymbol{V}$, and $\boldsymbol{V} = \dfrac{E[\Delta\boldsymbol{X}(\Delta\boldsymbol{X})^{\mathrm{T}}]}{\Delta t}$. The elements of $\boldsymbol{W}(t)$ are Wiener processes: each is normally distributed with mean zero and variance t. Matrix $\mathbf{H} \in \mathbb{R}^{\mathbf{3}\times\mathbf{6}}$ is composed of two submatrices, $\mathbf{H} = [\boldsymbol{\Sigma}_1 \mid \boldsymbol{\Sigma}_2]$, where

$$\boldsymbol{\Sigma}_1 = \begin{bmatrix} \sqrt{\mathcal{B}(\sigma(t), N)N + \mathcal{D}(\sigma(t), N)S} & 0 & 0 \\ 0 & \sqrt{\mathcal{D}_I(\sigma(t), N)I} & 0 \\ 0 & 0 & \sqrt{\mathcal{D}(\sigma(t), N)R} \end{bmatrix},$$

$$\boldsymbol{\Sigma}_2 = \begin{bmatrix} -\sqrt{\beta IS + \alpha\gamma I} & -\sqrt{vS} & 0 \\ \sqrt{\beta IS + \alpha\gamma I} & 0 & -\sqrt{(1-\alpha)\gamma I} \\ 0 & \sqrt{vS} & \sqrt{(1-\alpha)\gamma I} \end{bmatrix}.$$

Elements of vector $\boldsymbol{W}(t) = [W_1, W_2, W_3, W_4, W_5, W_6]^{\mathrm{T}}$ correspond to the columns of $\mathbf{H}$. The SDE model equations can be expressed component-wise:

$$\begin{aligned}
\mathrm{d}S &= \left[\mathcal{B}(\sigma(t), N)N + \alpha\gamma I - \left(\mathcal{D}(\sigma(t), N) + v + \beta I\right)S\right]\mathrm{d}t + \sqrt{\mathcal{B}(\sigma(t), N)N + \mathcal{D}(\sigma(t), N)S}\,\mathrm{d}W_1 \\
&\quad - \sqrt{\beta IS + \alpha\gamma I}\,\mathrm{d}W_4 - \sqrt{vS}\,\mathrm{d}W_5, \\
\mathrm{d}I &= \left[\beta IS - \left(\mathcal{D}_I(\sigma(t), N) + \gamma\right)I\right]\mathrm{d}t + \sqrt{\mathcal{D}_I(\sigma(t), N)I}\,\mathrm{d}W_2 - \sqrt{(1-\alpha)\,\gamma I}\,\mathrm{d}W_6 \\
&\quad + \sqrt{\beta IS + \alpha\gamma I}\,\mathrm{d}W_4, \\
\mathrm{d}R &= \left[vS + (1-\alpha)\gamma I - \mathcal{D}(\sigma(t), N)R\right]\mathrm{d}t + \sqrt{\mathcal{D}(\sigma(t), N)R}\,\mathrm{d}W_3 + \sqrt{vS}\,\mathrm{d}W_5 + \sqrt{(1-\alpha)\,\gamma I}\,\mathrm{d}W_6.
\end{aligned}$$

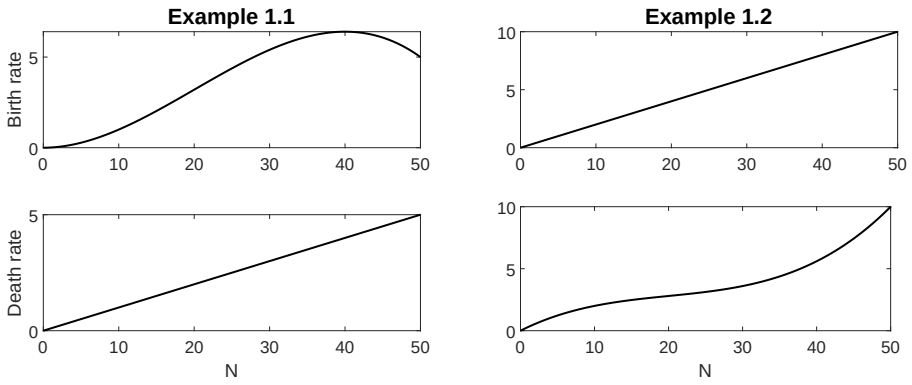

FIGURE 1. Birth and death rates for Example 1.1 and 1.2.

3. EXAMPLES

In this section, we discuss some models for $\mathcal{B}(\sigma(t), N)$, $\mathcal{D}(\sigma(t), N)$, and $\mathcal{D}_I(\sigma(t), N)$ that can produce two stable equilibria in the SIR model. We start with a general Allee effect model and then discuss three models with demographic parameters reflecting real populations. Our primary interest is to simulate a disease-induced extinction. By considering some example sets of disease parameters, we demonstrate that a stable population can collapse due to the spread of a disease. Whenever either $\sigma(t)$ or N is not a part of $\mathcal{B}(\sigma(t), N)$ or $\mathcal{D}(\sigma(t), N)$, we drop the corresponding variable for notational simplicity.

Example 3.1. To yield a simple mathematical equation that exhibits alternative stable states without a resource indicator function, we set the per-capita population growth rate $\mathcal{B}(N) - \mathcal{D}(N) = a_1 N - a_2 N^2 - d$ and $\mathcal{D}_I(N) - \mathcal{D}(N) = d_I - d$, where $a_1 = \dfrac{d}{k_1} + \dfrac{d}{k_2}$, $a_2 = \dfrac{d}{k_1 k_2}$, $d_I \geq d$, and $k_1 < k_2$. When $d_I = d$, this yields

$$\frac{\mathrm{d}N}{\mathrm{d}t} = dN\left(\frac{N}{k_1} - 1\right)\left(1 - \frac{N}{k_2}\right), \tag{3.1}$$

which is the common model for strong Allee effects [46, 47]. Note that if $\mathcal{B}(N)$, $\mathcal{D}(N)$, and $\mathcal{D}_I(N)$ are chosen to be polynomials of N, then all of them satisfy assumptions $\mathcal{A}2$ and $\mathcal{A}3$. Since $\mathcal{B}(0) - \mathcal{D}(0) = -d < 0$, the origin is locally stable. For simulations, consider a hypothetical population with a growth rate that can be modeled by the cubic function given by: $f(N) = 0.012N^2 - 0.1N - 0.0002N^3$. Here, N represents the number of animals per unit area. This function describes several key features:

1. The carrying capacity is 50 animals per unit area.
2. The critical population for a positive growth rate is 10 animals per unit area.
3. The maximum growth rate of 2.4 per unit time occurs when $N = 30$.

Many birth and death functions can produce such a growth rate. Below are two such examples. See Figure 1 for the corresponding birth and death rates.

1. (Example 1.1) A constant per-capita death rate $\mathcal{D}(N) = 0.1$ with a quadratic per-capita birth rate $\mathcal{B}(N) = 0.012N - 0.0002N^2$.
   (a) The birth rate $N\mathcal{B}(N)$ decreases near the carrying capacity due to resource limitations.
   (b) The death rate $N\mathcal{D}(N)$ is primarily determined by average life expectancy.
2. (Example 1.2) A constant per-capita birth rate $\mathcal{B}(N) = 0.2$ with a quadratic per-capita death rate $\mathcal{D}(N) = 0.3 - 0.012N + 0.0002N^2$.
   (a) The birth rate $N\mathcal{B}(N)$ does not depend on resource limitations.

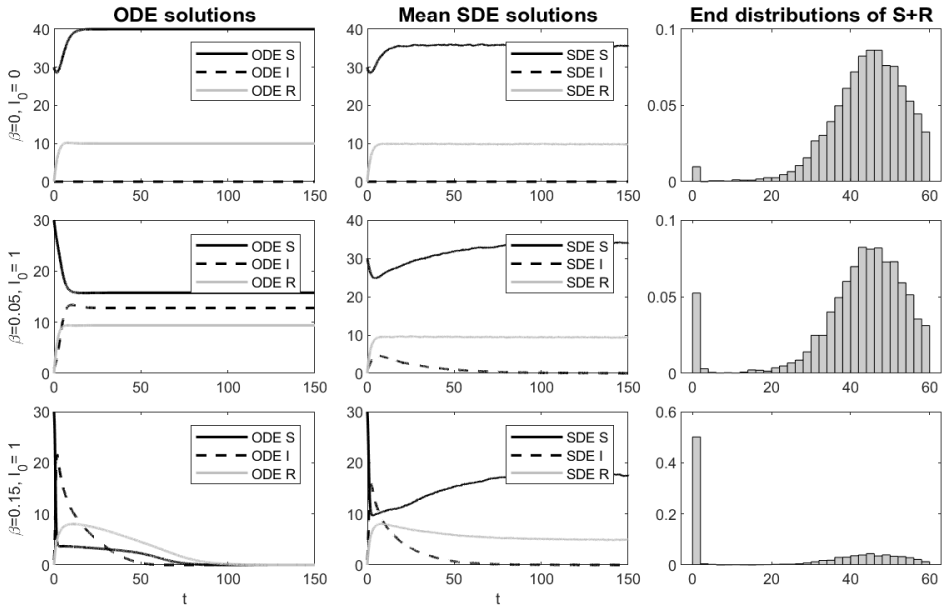

FIGURE 2. Solution curves for classes $S(t)$, $I(t)$ and $R(t)$ in Example 3.1 with ODE solutions (first column), the mean SDE solution from 5000 sample paths (second column), and the end distribution of $S(t) + R(t)$ (third column). The top row represents the disease-free solution with $(S_0, I_0, R_0) = (30, 0, 0)$, the middle row represents the endemic solution with $\beta = 0.05$ and $(S_0, I_0, R_0) = (30, 1, 0)$, and the bottom row shows a collapsed ODE population when $\beta = 0.15$ and $(S_0, I_0, R_0) = (30, 1, 0)$. Simulations are for 150 months and the discretization used in the simulations is $\Delta t = 0.01$.

(b) The slope of the death rate $N\mathcal{D}(N)$ increases near the carrying capacity, representing resource limitations.

We set the disease parameters to $(\alpha, \gamma, v, d_I) = (0.5, 0.2, 0.15, 0.3)$. This parameter set represents a disease with a higher death rate than the natural death rate and a partially immune population. We vary β to guarantee an endemic state ($R_0 > 1$) and observe the disease-induced stable states.

As we see in Figure 2, the mean of the stochastic model realizations need not be similar to the ODE solution. Without any disease, both models produce a stable positive population. When $\beta = 0.05$, the deterministic model produces a stable endemic state, whereas almost all the stochastic simulations produce a disease-free state. When $\beta = 0.15$, the deterministic model population collapses, as do about 50% of the stochastic sample path populations. However, the remaining sample paths result in a disease-free population. While this model provides a simulation platform to demonstrate disease-induced state changes, it may be difficult to adapt the model to real populations due to the existence of many other factors that influence demographic rates.

Example 3.2. The next model applies to populations that exhibit reduced reproduction at lower densities combined with a relatively constant birth rate at high densities. We then simulate the impact of including a birth season to observe a disease-induced extinction. Let $\sigma(t) = 1_U(t)$, where 1_U is the indicator function and U is the birthing season. Set $\mathcal{B}(\sigma(t), N) = \sigma(t)bN/(N + k)$, where b, k are positive constants. It is easy to see that $\sigma(t)$ satisfies Assumption $\mathcal{A}_1$. As a function of $\sigma(\cdot)$, $\mathcal{B}(\sigma(\cdot), N)$ is continuous and monotone increasing and, for $\sigma(t) = 1$, $\partial\mathcal{B}(1, N)/\partial N \in [0, b/k]$. Subsequently, Assumption $\mathcal{A}_2$ is satisfied. Assuming the growth rate reflects a carrying capacity (as in the logistic equation), we may choose linear per capita death functions $\mathcal{D}(N) = d + cN$ and $\mathcal{D}_I(N) = d_I + cN$, where d, d_I, c are positive constants and $d_I \geq d$. Functions $\mathcal{D}(N)$ and $\mathcal{D}_I(N)$ readily satisfy Assumption $\mathcal{A}_3$. Since $\mathcal{B}(0) - \mathcal{D}(0) = -d < 0$, the origin is locally stable.

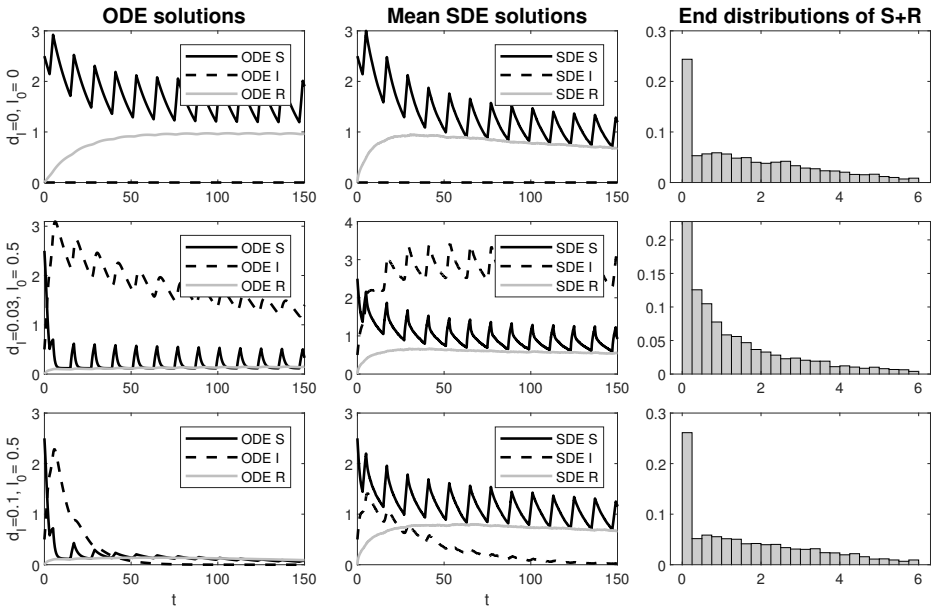

FIGURE 3. Solution curves for classes $S(t)$, $I(t)$ and $R(t)$ in Example 3.2 with ODE solutions (first column), the mean SDE solution of 5000 sample paths (second column), and the end distribution of $S(t) + R(t)$ (third column). The top row represents the disease-free solution with $(S_0, I_0, R_0) = (2.5, 0, 0)$, the middle row represents the endemic solution with $d_I = 0.03$ and $(S_0, I_0, R_0) = (2.5, 0.5, 0)$, and the bottom row shows a collapsed ODE population when $d_I = 0.1$ and $(S_0, I_0, R_0) = (2.5, 0.5, 0)$. Simulations are for 150 months and the discretization used in the simulations is $\Delta t = 0.005$.

We use Black tailed prairie dogs as a model species for simulations. Using data from [11], $1_U = 1$ for March and April, $b = 0.217$ per month, $d = 0.274$ per year, $c = 0.0178$ per year, and $k = 0.3$. For simulations, we set $\alpha = 1$ and $\gamma = 0.05$ per month so that only a fraction of the infected population recovers. Diseases such as Sylvatic plague are fatal for almost all who become infected [48]. We set $\beta = 0.4$ and $v = 0.02$ and vary d_I to obtain the simulation results for the deterministic and stochastic models (see Fig. 3).

When $I_0 = 0$, both the ODE and the mean of the SDE simulations produce a stable population. However, about 25% of the stochastic simulation sample paths converge to zero even without the disease and the corresponding mean is smaller than the ODE solution. While we find an endemic equilibrium population for $d_I = 0.03$ for both models, the SDE sample paths are apt to converge to a larger uninfected population compared to the ODE solution. At $d = 0.1$, ODE solution curves collapse. While about 25% of the SDE sample paths converge to zero, the majority converge to a disease-free state.

Example 3.3. Models for $\mathcal{B}(\sigma(\cdot), N)$ and $\mathcal{D}(\sigma(\cdot), N)$ can be more complicated than density dependent Allee effect models, as observable species characteristics and abiotic factors may influence the rates. The total body weight of herbivore mammals has a significant correlation to reproduction [31–33, 49]. The per capita mean recruitment rate of weaned juveniles to a population of such mammals may be represented by $\mathcal{B}(m, p) = \dfrac{\alpha_1(m - m^*)p}{\alpha_2(m - m^*) + 1}$ per year, where m is the mean body mass of the female population, p represents the proportion of juveniles surviving to weaning age, α_1, α_2, m^* are positive constants, and $m \geq m^*$ [28]. If a disease persists in a region for a long time, one could use either m or p as $\sigma(t)$. Function $\mathcal{B}(m, p)$ is continuously differentiable, $\partial\mathcal{B}(m, p)/\partial m = \alpha_1 p/(\alpha_2(m - m^*) + 1)^2 > 0$ and $\partial\mathcal{B}(m, p)/\partial p = \alpha_1(m - m^*)/(\alpha_2(m - m^*) + 1) > 0$. Therefore, $\mathcal{B}(m, p)$ satisfies assumption $\mathcal{A}2$ with respect to either variable. As in Example 3.2, we may define $\mathcal{D}(N) = d + cN$

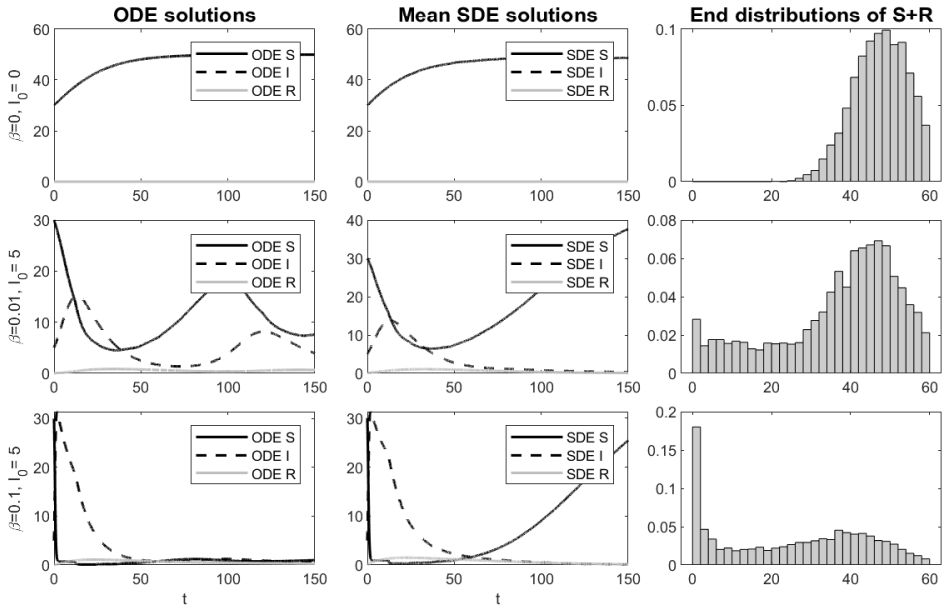

FIGURE 4. Solution curves for classes $S(t)$, $I(t)$ and $R(t)$ in Example 3.3 with ODE solutions (first column), the mean SDE solution of 5000 sample paths (second column), and the end distribution of $S(t) + R(t)$ (third column). The top row represents the disease-free solution with $(S_0, I_0, R_0) = (30, 0, 0)$, the middle row represents the endemic solution with $\beta = 0.01$ and $(S_0, I_0, R_0) = (30, 5, 0)$, and the bottom row shows a collapsed ODE population when $\beta = 0.1$ and $(S_0, I_0, R_0) = (30, 5, 0)$. Simulations are for 150 months and the discretization used in the simulations is $\Delta t = 0.01$.

and $\mathcal{D}_I(N) = d_I + cN$, where $d, c, d_I > 0$ and $d_I \geq d$. Whenever $\mathcal{B}(m, p) - \mathcal{D}(0) = \alpha_1(m - m^*)p/(\alpha_2(m - m^*) + 1) - d < 0$, the origin is locally stable.

For this example, we use white-tailed deer as a model species for simulations. In a healthy, well-managed deer population, we do not expect to see any Allee effects. However, a disease, such as Chronic Wasting Disease (CWD), alters the mean body weight of does, the survival rate of fawns to weaning age, and the mean survival rate of the population [34, 35, 50]. These changes in dynamics can result in a disease-induced Allee effect. Consider a population that is confined during the birth season to a 10km^2 region with an ecological carrying capacity of 50 per 10km^2. As in [28], for hardiness zone 5, we set $m^* = 25\text{kg}$, $\alpha_1 = 0.223$, $\alpha_2 = 0.0865$. With the linear per capita death function $\mathcal{D}(N) = d + cN$ and a 5-year of mean life expectancy, we obtain $d = 0.2$ per year and $c = 0.0136$ per individual per year to represent a carrying capacity of 50 per 10km^2 for a mean body weight of 50kg and $p = 0.5$. Consider the spread of a disease that impacts the survival rate of fawns to weaning age so that $\sigma(t) = p$. We assume that $\sigma(t)$ is a constant for each year and $\sigma(t) = (1 - \rho_I(t))/2$, where $\rho_I(t)$ is the proportion of infected individuals at the beginning of year t. Although deer reproduce seasonally, we use the average model for simulation purposes. Note that we may also set $\sigma(t) = p1_U(t)$ to satisfy Assumption $\mathcal{A}2$, where U is the white-tailed deer birthing season.

Next we simulate the spread of a disease with parameters $\alpha = 0.5$ and $(\gamma, v, d_I) = (0.1, 0, 1.0)$ per year, representing a very low recovery rate: infected deer are 5 times more likely to die annually than uninfected deer. We also assume that no individual is vaccinated. Such a parameter set mimics diseases such as CWD, where CWD-positive deer were 4.5 times more likely to die annually than CWD-negative deer [34]. We fix β to guarantee an endemic state and observe the disease-induced stable states. Figure 4 summarizes the simulation results.

When there is no disease, both deterministic and mean stochastic solutions approach the population carrying capacity. At $\beta = 0.01$, the deterministic solution stays in an endemic state for at least the first 150 months, whereas the mean stochastic solution converges to a disease-free state. At $\beta = 0.1$, the deterministic solution collapses to produce an extinction. While the mean stochastic solution nearly reaches extinction at around 5 years, the simulations demonstrate that more than 75% of the sample paths recover to the disease-free solution.

Example 3.4. An significant feature of the generalized SIR model is its potential for incorporating regression models for the fitness components. As an example, we use the long-term population dynamics of pronghorns in Nebraska given by Hoffman *et al.* [51]. Let N be the pronghorn density in individuals per square kilometer. The per capita rate of change of pronghorn density among one of the management units (Banner region) discussed in [51] was modeled by $f(N)/N = 0.169\ln(N) - 0.0198$ per year for $0.3 \le N \le 2.7$, where $f(N)$ is the growth rate. Since $\ln(N) \to -\infty$ as $N \to 0$, this model cannot be directly utilized for studying a possible disease-driven extinction. We approximate $f(N)/N$ by a quadratic function using the method of least squares to obtain $\mathcal{B}(N,\sigma(t)) - \mathcal{D}(N,\sigma(t)) = 0.306N - 0.057N^2 - 0.279$, which yields a carrying capacity of 4.2 pronghorns/km^2. In fact, 4.26 individuals/km^2 was the maximum density observed in three out of four pronghorn management units during 1955-1993 [51]. In the wild, a pronghorn's lifespan is about 10 years, so we set the natural death rate to 0.1 [52]. Winter weather severity (as measured by snow depth) has best explained the annual pronghorn mortality risk [38]. Therefore, we set $\sigma(t) = -s(t)$ and $\mathcal{D}(N,\sigma(t)) = 0.1 + k_1(s(t) - k_2) + cN^2$, where $s(t)$ is the annual snowfall (in cm) in western Nebraska and $c, k_1, k_2 > 0$. Assuming the average annual snowfall is 80cm, the birth function is linear, $\mathcal{D}(0,0) = 0.1$, and no strong Allee effect is exhibited when $s(t) < 30$, we obtain $\mathcal{B}(N) = 0.306N + 0.2674$ and $\mathcal{D}(N,\sigma(t)) = 0.1 + 0.00558s(t) + 0.057N^2$. Since both $\mathcal{B}(N)$ and $\mathcal{D}(N,\sigma(t))$ are continuously differentiable with respect to N and $\partial\mathcal{D}(N,\sigma(t))/\partial\sigma = -0.00558$, both functions satisfy the conditions in Assumptions $\mathcal{A}_2$ and $\mathcal{A}_3$. Since $\mathcal{B}(0) - \mathcal{D}(0,\sigma) = 0.1674 - 0.00558s(t)$, the origin is locally stable for $s(t) > 30$.

Next we simulate the impact of snow depth on disease dynamics when there is an immune subpopulation. We consider $s(t) = 75$ cm both with and without an infected population and $s(t) = 100$ cm with an infected population. We set $\mathcal{D}_I(N,\sigma(t)) = 0.5 + 0.00558s(t) + 0.057N^2$, $\alpha = 0$, and $(\beta,\gamma,v) = (0.15, 0.05, 0.05)$ per month. With this parameter set, we assume that all recovered individuals are immune and the infected population has a higher mortality rate than the susceptible population. With the chosen $\mathcal{D}_I(N,\sigma(t))$, an infected pronghorn is 1.75 times more likely to die than a uninfected one at $s(t) = 75$ cm. Figure 5 summarizes the simulation results.

In the absence of the disease, the density $S + R$ corresponding to the ODE solution converges to the carrying capacity, 4.2 pronghorns/km^2. However, the mean $S + R$ SDE solution stays around 1.5 pronghorns/km^2, which is much closer to the average density in the Banner Unit during 1955-1993 (1.3 pronghorns/km^2). When the disease is introduced, the ODE solution converges to a stable endemic state, whereas the mean SDE solution converges to the disease-free state with an end distribution that is almost identical to the case without the disease. When $s(t) = 100$ cm, ODE solution and about 65% of the stochastic sample paths show a population collapse.

4. Conclusion

In this paper, we discuss disease-induced extinction influenced by temporal variations in reproduction and mortality rates. Density-dependent models alone may not be able to predict the potential for extinction, as fluctuations in resource limitations and allocations can directly impact a population's collapse. These variations can be induced by density and seasonality (Examples 3.1 and 3.2), the disease itself (Example 3.3), or fluctuations in summer and winter weather (Example 3.4). One can model the reproduction and mortality rates by including various indicators to incorporate these factors. We demonstrate that a discrete time series of external observations reflecting temporal variations can be sufficiently incorporated into disease models as piecewise constant functions.

The primary achievement of this work is to establish the framework for integrating field observations and associated regression models, encompassing various parameters directly into epidemic models. This allows us

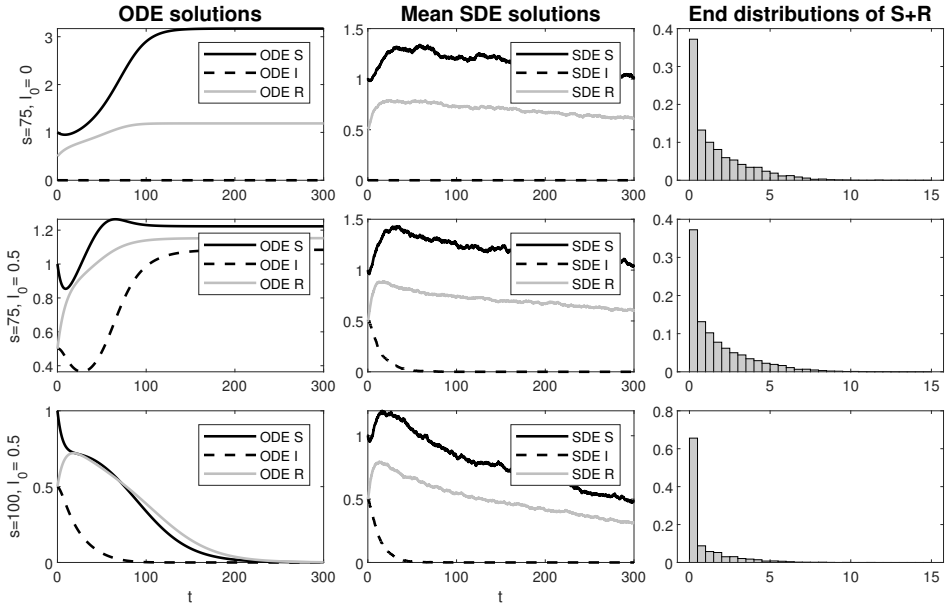

FIGURE 5. Solution curves for classes $S(t)$, $I(t)$ and $R(t)$ in Example 3.4 with ODE solutions (first column), the mean SDE solution of 5000 sample paths (second column), and the end distribution of $S(t) + R(t)$ (third column). The top row represents the disease-free solution with $s(t) = 75$cm and $(S_0, I_0, R_0) = (1, 0, 0.5)$, the middle row represents the endemic solution with $s(t) = 75$cm and $(S_0, I_0, R_0) = (1, 0.5, 0.5)$, and the bottom row shows a collapsed ODE population when $s(t) = 100$cm and $(S_0, I_0, R_0) = (1, 0.5, 0.5)$. Simulations are for 300 months and the discretization used in the simulations is $\Delta t = 0.01$.

to assess and predict the resultant solution paths over time. Such results are valuable for identifying effective disease management and prevention strategies, especially when external variables such as climate patterns impact disease spread and potential extinctions. While we introduce incorporating field observations in the birth and death functions, a future direction for extending this work could be to similarly incorporate external observations on transmission and recovery parameters.

ACKNOWLEDGEMENTS

The authors wish to thank anonymous reviewers for their helpful comments.

REFERENCES

[1] R.C. Lewontin, The meaning of stability. *Diversity Stabil. Ecol. Syst.* **22** (1969) 13–24.
[2] B.E. Beisner, D.T. Haydon and K. Cuddington, Alternative stable states in ecology. *Front. Ecol. Environ.* **1** (2003) 376–382.
[3] C. Folke, S. Carpenter, B. Walker, M. Scheffer, T. Elmqvist, L. Gunderson and C.S. Holling, Regime shifts, resilience, and biodiversity in ecosystem management. *Annu. Rev. Ecol. Evol. Syst.* **35** (2004) 557–581.
[4] I.A. van de Leemput, V. Dakos, M. Scheffer and E.H. van Nes, Slow recovery from local disturbances as an indicator for loss of ecosystem resilience. *Ecosystems* **21** (2018) 141–152.
[5] K.N. Suding, K.L. Gross and G.R. Houseman, Alternative states and positive feedbacks in restoration ecology. *Trends Ecol. Evol.* **19** (2004) 46–53.
[6] F. De Castro and B. Bolker, Mechanisms of disease-induced extinction. *Ecol. Lett.* **8** (2005) 117–126.
[7] K.E. Emmert and L.J.S. Allen, Population extinction in deterministic and stochastic discrete-time epidemic models with periodic coefficients with applications to amphibian populations. *Nat. Resource Model.* **19** (2006) 117–164.

[8] H.R. Thieme, T. Dhirasakdanon, Z. Han and R. Trevino, Species decline and extinction: synergy of infectious disease and allee effect? *J. Biol. Dyn.* **3** (2009) 305–323.

[9] Y. Kang and C. Castillo-Chavez, Multiscale analysis of compartment models with dispersal. *J. Biol. Dyn.* **6** (Suppl. 2)(2012) 50–79.

[10] A. Friedman and A.-A. Yakubu, Host demographic Allee effect, fatal disease, and migration: Persistence or extinction. *SIAM J. Appl. Math.* **72** (2012) 1644–1666.

[11] A.J. Ekanayake and D.B. Ekanayake, A seasonal sir metapopulation model with an Allee effect with application to controlling plague in prairie dog colonies. *J. Biol. Dyn.* **9** (Supp1.) (2015) 262–290.

[12] W.C. Allee, The Social Life of Animals. New York, W.W. Norton & Company, Inc. (1938).

[13] F. Courchamp, L. Berec and J. Gascoigne, Allee Effects in Ecology and Conservation. OUP, Oxford (2008).

[14] K.R. Hopper and R.T. Roush, Mate finding, dispersal, number released, and the success of biological control introductions. *Ecol. Entomol.* **18** (1993) 321–331.

[15] H.G. Davis, C.M. Taylor, J.G. Lambrinos and D.R. Strong, Pollen limitation causes an Allee effect in a wind-pollinated invasive grass (Spartina alterniflora). *Proc. Natl. Acad. Sci. U.S.A.* **101** (2004) 13804–13807.

[16] K.-H. Choi and W.J. Kimmerer, Mate limitation in an estuarine population of copepods. *Limnol. Oceanogr.* **53** (2008) 1656.

[17] M.S. Mooring, T.A. Fitzpatrick, T.T. Nishihira and D.D. Reisig, Vigilance, predation risk, and the allee effect in desert bighorn sheep. *J. Wildlife Manag.* **68** (2004) 519–532.

[18] K.H. Elliott, G.S. Betini and D.R. Norris, Fear creates an Allee effect: experimental evidence from seasonal populations. *Proc. Roy. Soc. B: Biol. Sci.* **284** (2017) 20170878.

[19] S.A. West, A.S. Griffin and A. Gardner, Social semantics: altruism, cooperation, mutualism, strong reciprocity and group selection. *J. Evol. Biol.* **20** (2007) 415–432.

[20] P.A. Stephens and W.J. Sutherland, Consequences of the Allee effect for behaviour, ecology and conservation. *Trends Ecol. Evol.* **14** (1999) 401–405.

[21] E. Angulo, G.M. Luque, S.D. Gregory, J.W. Wenzel, C. Bessa-Gomes, L. Berec and F. Courchamp, Allee effects in social species. *J. Anim. Ecol.* **87** (2018) 47–58.

[22] J.-M. Gaillard, M. Festa-Bianchet and N.G. Yoccoz, Population dynamics of large herbivores: variable recruitment with constant adult survival. *Trends Ecol. Evol.* **13** (1998) 58–63.

[23] J.M. Gaillard, M. Festa-Bianchet, N.G. Yoccoz, A. Loison and C. Toigo, Temporal variation in fitness components and population dynamics of large herbivores. *Annu. Rev. Ecol. Syst.* **31** (2000) 367–393.

[24] L.L. Eberhardt, A paradigm for population analysis of long-lived vertebrates. *Ecology* **83** (2002) 2841–2854.

[25] C. Bonenfant, J.-M. Gaillard, T. Coulson, M. Festa-Bianchet, A. Loison, M. Garel, L.E. Loe, P. Blanchard, N. Pettorelli, N. Owen-Smith, *et al.*, Empirical evidence of density-dependence in populations of large herbivores. *Adv. Ecol. Res.* **41** (2009) 313–357.

[26] K.L. Monteith, V.C. Bleich, T.R. Stephenson, B.M. Pierce, M.M. Conner, J.G. Kie and R.T. Bowyer, Life-history characteristics of mule deer: effects of nutrition in a variable environment. *Wildlife Monogr.* **186** (2014) 1–62.

[27] E.J. Chapman and C.J. Byron, The flexible application of carrying capacity in ecology. *Global Ecol. Conserv.* **13** (2018) e00365.

[28] D.B. Ekanayake, A.J. Ekanayake, J. Hunt and C.L. Miller-Hunt, Modeling reproduction of whitetail deer and its applications. *J. Theor. Biol.* **459** (2018) 90–102.

[29] F. Valladares, D. Sanchez-Gomez and M.A. Zavala, Quantitative estimation of phenotypic plasticity: bridging the gap between the evolutionary concept and its ecological applications. *J. Ecol.* **94** (2006) 1103–1116.

[30] E.E. Werner and S.D. Peacor, A review of trait-mediated indirect interactions in ecological communities. *Ecology* **84** (2003) 1083–1100.

[31] R. Langvatn, S.D. Albon, T. Burkey and T.H. Clutton-Brock, Climate, plant phenology and variation in age of first reproduction in a temperate herbivore. *J. Anim. Ecol.* **65** (1996) 653–670.

[32] N. Pettorelli, J.-M. Gaillard, G. Van Laere, P. Duncan, P. Kjellander, O. Liberg, D. Delorme and D. Maillard, Variations in adult body mass in roe deer: the effects of population density at birth and of habitat quality. *Proc. Roy. Soc. Lond. Ser. B: Biol. Sci.* **269** (2002) 747–753.

[33] B.-E. Sæther and M. Heim, Ecological correlates of individual variation in age at maturity in female moose (*Alces alces*): the effects of environmental variability. *J. Anim. Ecol.* **62** (1993) 482–489.

[34] D.R. Edmunds, M.J. Kauffman, B.A. Schumaker, F.G. Lindzey, W.E. Cook, T.J. Kreeger, R.G. Grogan and T.E Cornish, Chronic wasting disease drives population decline of white-tailed deer. *PLoS One* **11** (2016) e0161127.

[35] R.J. Monello, J.G. Powers, N.T. Hobbs, T.R. Spraker, M.K. Watry and M.A. Wild, Survival and population growth of a free-ranging elk population with a long history of exposure to chronic wasting disease. *J. Wildlife Manag.* **78** (2014) 214–223.

[36] D.E. Brown, D. Warnecke and T. McKinney, Effects of midsummer drought on mortality of doe pronghorn (*Antilocapra americana*). *Southwest. Natural.* **51** (2006) 220–225.

[37] D.C. Simpson, L.A. Harveson, C.E. Brewer, R.E. Walser and A.R. Sides, Influence of precipitation on pronghorn demography in Texas. *J. Wildlife Manag.* **71** (2007) 906–910.

[38] P.F. Jones, A.F. Jakes, D.R. Eacker and M. Hebblewhite, Annual pronghorn survival of a partially migratory population. *J. Wildlife Manag.* **84** (2020) 1114–1126.

[39] L. Cai, G. Chen and D. Xiao, Multiparametric bifurcations of an epidemiological model with strong Allee effect. *J. Math. Biol.* **67** (2013) 185–215.

[40] Y. Liu, S. Ruan and L. Yang, Stability transition of persistence and extinction in an avian influenza model with Allee effect and stochasticity. *Commun. Nonlinear Sci. Numer. Simul.* **91** (2020) 105416.

[41] R. Lande, Genetics and demography in biological conservation. *Science* **241** (1988) 1455–1460.

[42] J.K. Hale, Ordinary Differential Equations. Dover (1980).

[43] J.M. Heffernan, R.J. Smith and L.M. Wahl, Perspectives on the basic reproductive ratio. *J. Roy. Soc. Interface* **2** (2005) 281–293.

[44] D. Serre, Matrices: Theory and Applications. Springer (2010).

[45] E. Allen, editor, *Modeling with Itô Stochastic Differential Equations*. Mathematical Modelling: Theory and Applications. Springer (2007).

[46] F.M. Hilker, M. Langlais and H. Malchow, The Allee effect and infectious diseases: extinction, multistability, and the (dis-) appearance of oscillations. *Am. Natural.* **173** (2009) 72–88.

[47] A. Friedman and A.-A. Yakubu, Fatal disease and demographic Allee effect: population persistence and extinction. *J. Biol. Dyn.* **6** (2012) 495–508.

[48] J.F. Cully Jr. and E.S. Williams, Interspecific comparisons of sylvatic plague in prairie dogs. *J. Mammal.* **82** (2001) 894–905.

[49] T.M. Blackburn, K.J. Gaston and N. Loder, Geographic gradients in body size: a clarification of Bergmann's rule. *Diversity Distrib.* **5** (1999) 165–174.

[50] A.N. Hamir, R.A. Kunkle, E.M. Nicholson, J.M. Miller, S.M. Hall, H. Schoenenbruecher, B.W. Brunelle and J.A. Richt, Preliminary observations on the experimental transmission of chronic wasting disease (CWD) from elk and white-tailed deer to fallow deer. *J. Compar. Pathol.* **138** (2008) 121–130.

[51] J.D. Hoffman, H.H. Genoways and R.R. Jones, Factors influencing long-term population dynamics of pronghorn (*Antilocapra americana*): evidence of an Allee effect. *J. Mammal.* **91** (2010) 1124–1134.

[52] B. Grzimek, Grzimek's Encyclopedia of Mammals. McGraw-Hill (1990).